



# ARCHIVES of FOUNDRY ENGINEERING

ISSN (2299-2944)  
Volume 2022  
Issue 3/2022

60 – 66

10.24425/afe.2022.140237

8/3



Published quarterly as the organ of the Foundry Commission of the Polish Academy of Sciences

# The Influence of Optimization Parameters on the Efficiency of Aluminium Melt Refining by using Physical Modelling

J. Walek \* , K. Michalek , M. Tkadlečková 

VŠB - Technical University of Ostrava, Faculty of Materials Science and Technology,  
Department of Metallurgical Technologies, Czech Republic

\* Corresponding author. E-mail address: josef.walek@vsb.cz

Received 08.03.2022; accepted in revised form 01.06.2022; available online 07.09.2022

## Abstract

The article describes the influence of optimization parameters on the efficiency of aluminium melt refining by using physical modelling. The blowing of refining gas, through a rotating impeller into the ladle is a widely used operating technology to reduce the content of impurities in molten aluminium, e.g. hydrogen. The efficiency of this refining process depends on the creation of fine bubbles with a high interphase surface, wide-spread distribution, the residence time of its effect in the melt, and mostly on the wide-spread dispersion of bubbles in the whole volume of the refining ladle and with the long period of their effect in the melt. For physical modelling, a plexiglass model on a scale of 1:1 is used for the operating ladle. Part of the physical model is a hollow shaft used for gas supply equipped with an impeller and also two baffles. The basis of physical modelling consists in the targeted utilization of the similarities of the processes that take place within the actual device and its model. The degassing process of aluminium melt by blowing inert gas is simulated in physical modelling by a decrease of dissolved oxygen in the model liquid (water).

**Keywords:** Physical modelling, Refining ladle, Blowing of inert gas, Degassing of the melt, Impeller

## 1. Introduction

The use of aluminium alloys in the current product portfolio is constantly growing. With the growing demand, much more emphasis is placed on the quality of these products. The basic and most used process for improving the quality of aluminium alloys is aluminium refining. One of the most used and efficient technologies is degassing using so-called rotary refining. The method of blowing inert gas, so-called refining gas, through a rotating impeller into the ladle presents the most common operational technology in order to reduce the content of impurities in a molten aluminium, e.g., hydrogen [1-5].

The degassing technology by using inert gas is based on the Sieverts Law. It is possible to reduce the gas content in the melt by reducing its partial pressure in an inert gas bubble, according to the Sieverts Law. The main optimization parameters are the rotary impeller speed and the amount of blown inert gas [6-7].

The optimization of the degassing process is difficult under operating conditions. Therefore, in laboratory conditions, so-called modelling is used, where the original prototype is replaced by a model. The technology of modelling is divided into two basic methods. In numerical modelling, the process is described by a mathematical model that is formed of a system of partial differential equations. In the case of physical modelling, a method is used, in which the real system is replaced by



© The Author(s) 2022. Open Access. This article is licensed under a Creative Commons Attribution 4.0 International License (<http://creativecommons.org/licenses/by/4.0/>), which permits use, sharing, adaptation, distribution and reproduction in any medium or format, as long as you give appropriate credit to the original author(s) and the source, provide a link to the Creative Commons licence, and indicate if changes were made.

a tangible physical model, which is as close as most closely resembles a real device. Fluid flow in the technological process is thus modeled again by fluid flow in the model, but in a certain scale of lengths, volume flow rates, viscosities, etc. The condition for transferring results from the model on the prototype is the similarity of the processes taking place in the model and the prototype. One of the advantages of physical modelling is the possibility of visualising processes that contribute to understanding the processes taking place in real systems. The results achieved on the model can predict the real system behaviour in the course of various process changes. The combination of physical and numerical modelling is an optimal model research variant [8-11].

Among the biggest consumers of aluminum alloys include the engineering and automotive industries. In some applications, they can also replace structural steel. This alternative will achieve the preferred ratio of low density and good mechanical properties [12-13].

The aim of our research work using the method of physical modelling was to assess the influence of relevant technological parameters on the degassing process of the bath when blowing inert gas through a rotating impeller.

## 2. Performed experiments of physical modelling

Physical modelling was performed in the Laboratory of Physical and Numerical Modelling of the Department of Metallurgy and Foundry, Faculty of Materials Science and Technology. This laboratory is located on the premises of the Innovation Support Centre on the campus of the VSB – Technical University of Ostrava. The physical model was made of transparent organic glass (plexiglass) on a 1:1 scale to the real equipment (prototype) for the refining of molten aluminium with a ladle inner diameter of 800 mm. Additionally, two graphite baffles for suppressing excessive surface ripple and vortex formation were included in the physical modelling. Figure 1 shows a device of the physical model. Figure 2 shows the basic dimensional data of the physical model, including the location of the measuring probes.

Two variants of impellers, referred to as F2A 190 and J8 190, were used for modelling (see Figure 3).

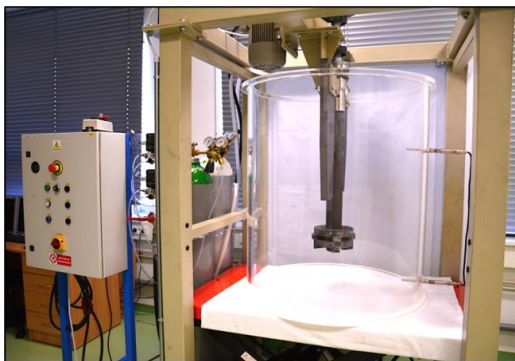


Fig. 1. Complete equipment of the physical model [10]

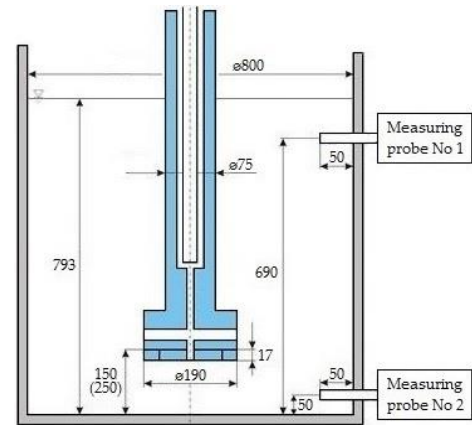


Fig. 2. Basic dimensional data of physical model [10]



Fig. 3. The impeller variants: (a) F2A 190, (b) J8 190

The physical model was placed on a lifting platform. This hydraulically controlled lifting platform made it possible to adjust the distance of the impeller from the bottom of the ladle. Rotary impeller speeds (revolutions per minute; rpm) were controlled by using an asynchronous motor, which was powered by the alternating current with variable frequency from an inverter. The model also included pressure bottles with oxygen and argon. Needle regulate valves, three-way valves, and mass flowmeters were used to measure and regulate the flow of gases – oxygen and argon [1].

The decrease of hydrogen content in molten aluminium during refining with inert gas is simulated in physical modelling by a decrease of dissolved oxygen in model liquid (water). The main advantage of using water is primarily its low cost, good availability and especially because it has similar physical properties as liquid aluminium. The dynamic viscosity of aluminium and water can be considered to be very close. Table 1 states the basic parameters of aluminium melt and water.

Table 1.

Comparison of basic physical parameters of the aluminium melt and water [1, 10]

Parameter	Aluminium	Water
Temperature – T (K)	1023	293
Density – $\rho$ ( $\text{kg} \cdot \text{m}^{-3}$ )	2345	998.5
Kinematic visc. – $\nu$ ( $\text{m}^2 \cdot \text{s}^{-1}$ )	$0.51 \cdot 10^{-6}$	$1.012 \cdot 10^{-6}$
Dynamic visc. – $\eta$ ( $\text{kg} \cdot \text{m}^{-1} \cdot \text{s}^{-1}$ )	0.00120	0.00101
Surface tension – $\sigma$ ( $\text{N} \cdot \text{m}^{-1}$ )	0.680	0.072

Laboratory experiments were conducted in accordance with the theory of similarity between the model and the prototype, based on the identity of Froude's criterion. It is necessary to observe, in particular, geometrical similarity and the dynamic similarity of fluid. The first step of the experimental study is to set the required distance of the impeller from the bottom of the modelling ladle using a hydraulic platform, height adjustment of the baffles. Subsequently, the refining ladle is filled with water at a temperature of 293 K at a distance of 793 mm from the bottom of the model. Subsequently, all partial systems are activated, such as starting the inverter, connecting the power supply to the devices, starting a program on the computer for reading and registering the measured oxygen content. In the next phase, the water in the model is saturated with oxygen gas to exactly 23 ppm. Then the required rotary impeller speed, volume flow rate of argon are set and the experiment itself and data loading via PC are started. The experiment is terminated when the oxygen content of the water does not change. Two optical fluorescent probes were used for the continuous measurement of oxygen content in the model bath (water).

### 3. Experiments and their evaluation

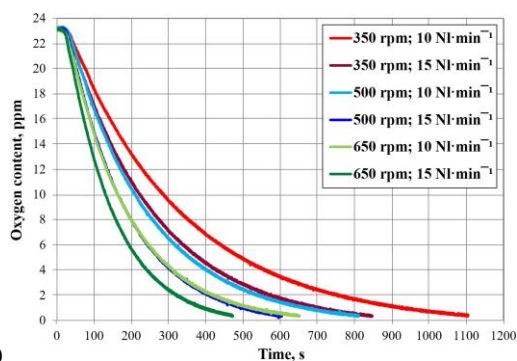
The main aim of physical modelling was to achieve insight into the effect of relevant parameters (see Table 2) on the removal of dissolved oxygen during refining. The research concentrated on the impeller variant, the distance of the impeller from the bottom of the refining ladle, flow rate of inert gas and rotary impeller speeds.

Table 2.

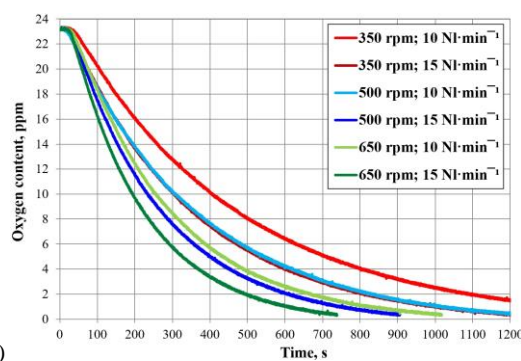
Overview of experimental conditions for physical modelling

Impeller variant	F2A 190	J8 190
Distance of the impeller (mm)	150	150
	250	250
Volume flow rate of Ar (Nl·m <sup>-1</sup> )	10	10
	15	15
Rotary impeller speeds (rpm)	350	350
	500	500
	650	650

The evaluation of the experiments was carried out in three phases. In the first phase, results were compared by the use of



a)



b)

Fig. 4. Influence of the change of volume flow rate of inert gas and rotary impeller speeds on the concentration of oxygen for the individual impellers: (a) F2A 190, (b) J8 190 [10]

combined graphs, in the second phase, the results were compared on the basis of the requirement for reaching a dimensionless concentration in the bath (in this case, 0.5 and 0.1) and, in the last evaluation phase, visualization photos were taken, where the size of bubbles and the distribution of these bubbles into the volume of the refining ladle were studied.

### 3.1. The comparison of experiments by use of combined graphs

The results of individual experiments were evaluated and processed into graphs, which characterise the time dependence of the evolution of the reduction of oxygen concentration during refining by inert gas.

As already mentioned, two optical fluorescent probes were used to measure the dissolved oxygen concentration in water (A1 – upper probe, A2 – lower probe). The analysis of the results revealed that the course of change in the oxygen concentration indicated by these probes is practically identical. This behaviour was evident in all experiments, due to the high rate of turbulence, which caused an almost homogeneous concentration field across the entire refining ladle model volume. Values from the lower probe A2 were used at the next evaluation due to this behaviour.

The influence of rotary impeller speeds and flow rate of inert gas was monitored for 350, 500, and 650 rpm values at a constant flow rate of inert gas of 10 and 15 Nl·min<sup>-1</sup> and the distance of the impeller from the bottom of the ladle of 150 mm. Figure 4 shows the graphs with the results of the individual impellers F2A 190 and J8 190. From the graphs that are shown below, a significant effect of increased rotary impeller speeds on the process of reduction of oxygen content is demonstrated. The increased flow rate of inert gas also has an influence. The dependence on gas rate can be seen in the different steepness of curves at the same rotary speed. The graphs show that it is possible to trace a simple connection between an increase in rotary speeds and the flow rate of inert gas. The same positive effect as the increase in rotary speeds by 150 rpm can also be approximately achieved by increasing the flow rate of inert gas from 10 to 15 Nl·min<sup>-1</sup> without changing the rotary speeds. It follows that the highest efficiency was achieved at a rotary speed of 650 rpm and a flow rate of inert gas of 15 Nl·min<sup>-1</sup>.

The distance of the impeller from the bottom of the ladle has a very important effect on the promotion of an even distribution of inert gas in the volume of the refined bath. At a greater distance from the bottom, the effect of refining may be less pronounced; at a shorter distance from the bottom, there may be a risk of increased lining erosion due to excessive turbulence and rotation of the bath near the bottom of the ladle. Figure 5 shows graphs documenting the effect of the distance between the impeller and

the bottom of the model for 150 and 250 mm, at a rotary speeds of 500 rpm and a volume flow rate of inert gas of 10 and 15  $\text{Nl}\cdot\text{min}^{-1}$ , for impellers F2A 190 and J8 190. The graphs presented below clearly show that the increase in the distance of the impeller from the bottom of the ladle from 150 to 250 mm was reflected in a decrease in refining efficiency, respectively, in increasing refining times. A similar course was confirmed at a rotary speeds 350 and 500 rpm.

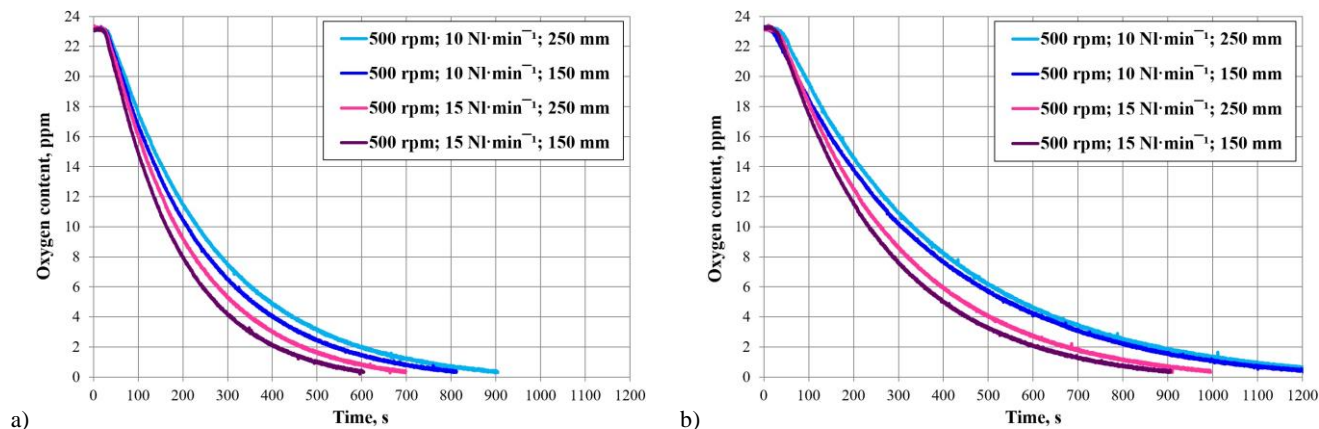


Fig. 5. Influence of the distance of the impeller above the bottom of the ladle on the concentration of oxygen for the impellers: (a) F2A 190, (b) J8 190 [10]

### 3.2. The comparison of the results based on time to reach the dimensionless concentration

For an easier interpretation and graphical comparison of the achieved results of the given experiments, the times  $\tau_{0.5}$  and  $\tau_{0.1}$  are compared. These times represent times under which the initial oxygen concentration in the bath was reduced at 50 % and 10 %, respectively, in other words, in which dimensionless concentrations  $C_x=0.5$  and  $C_x=0.1$  were achieved. The dimensionless concentration  $C_x$  is calculated, according to equation (1):

$$C_x = C_\tau / C_{\text{int}} \quad (1)$$

Where:

$C_\tau$  oxygen concentration in the bath (ppm)  
 $C_{\text{int}}$  initial concentration at beginning of the experiment (standardized to 23 ppm)

The time  $\tau_{0.5}$  and  $\tau_{0.1}$  is the time during which the original concentration of 23 ppm drops to 11.5 ppm and analogously to 2.3 ppm. Therefore, these parameters can characterise the rate of reduction of the content of oxygen dissolved in the bath.

Figure 6 shows a significant effect of rotary speeds and volume flow rate of inert gas on both values  $\tau_{0.5}$  (a) and  $\tau_{0.1}$  (b). As the rotary speeds (350, 500, 650 rpm) and flow rate (10, 15  $\text{Nl}\cdot\text{min}^{-1}$ ) increase, both  $\tau_{0.5}$  and  $\tau_{0.1}$  decrease. Again, there is a visible trend in which approximately the same positive effect as an increase in rotary speeds of 150 rpm at a constant flow rate can be achieved by increasing the flow rate of inert gas from 10 to 15  $\text{Nl}\cdot\text{min}^{-1}$  without changing the rotary speeds. From both graphs, it is also clear that the better results were achieved by the impeller F2A 190.

The obtained experimental data were checked and it can be said that the curves correspond to the exponential dependence of  $c=c_0 \cdot e^{kt}$  with an exponent in the range of -0.003 to -0.009. It can also be seen from the columnar graphs that the time  $\tau_{0.1}$  is three times higher than the time  $\tau_{0.5}$  in most variants.

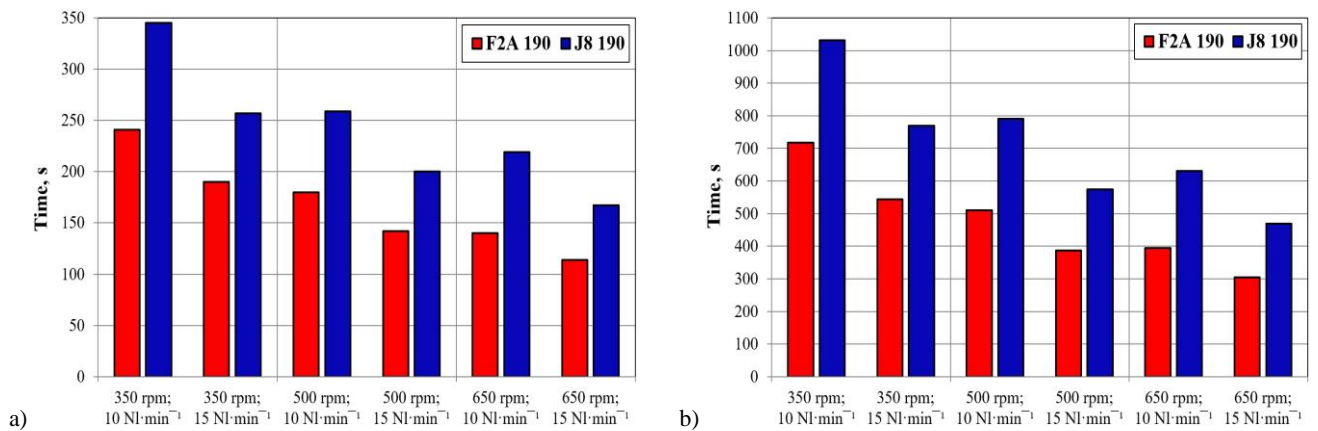


Fig. 6. Comparison of the influence of the impeller geometry, the volume flow rate of inert gas and the rotary impeller speeds on refining time at a constant distance of the impeller from the bottom of 150 mm on the values: (a)  $\tau_{0.5}$ , (b)  $\tau_{0.1}$

### 3.3. Visualization monitoring

During the experiments, photos of the bath behaviour inside the model were taken, from which the fluid flow and the amount and distribution of inert gas bubbles could be evaluated. The impellers F2A 190 and J8 190 were used for visualization, at

rotary speeds of 350, 500, and 650 rpm and a volume flow rate of inert gas of 10 and 15 NL·min<sup>-1</sup>. Figure 7 shows the selection of the bath behaviour using the above-mentioned impellers and a volume flow rate of inert gas of 10 NL·min<sup>-1</sup> at the distance of the impeller from the bottom of 150 mm.

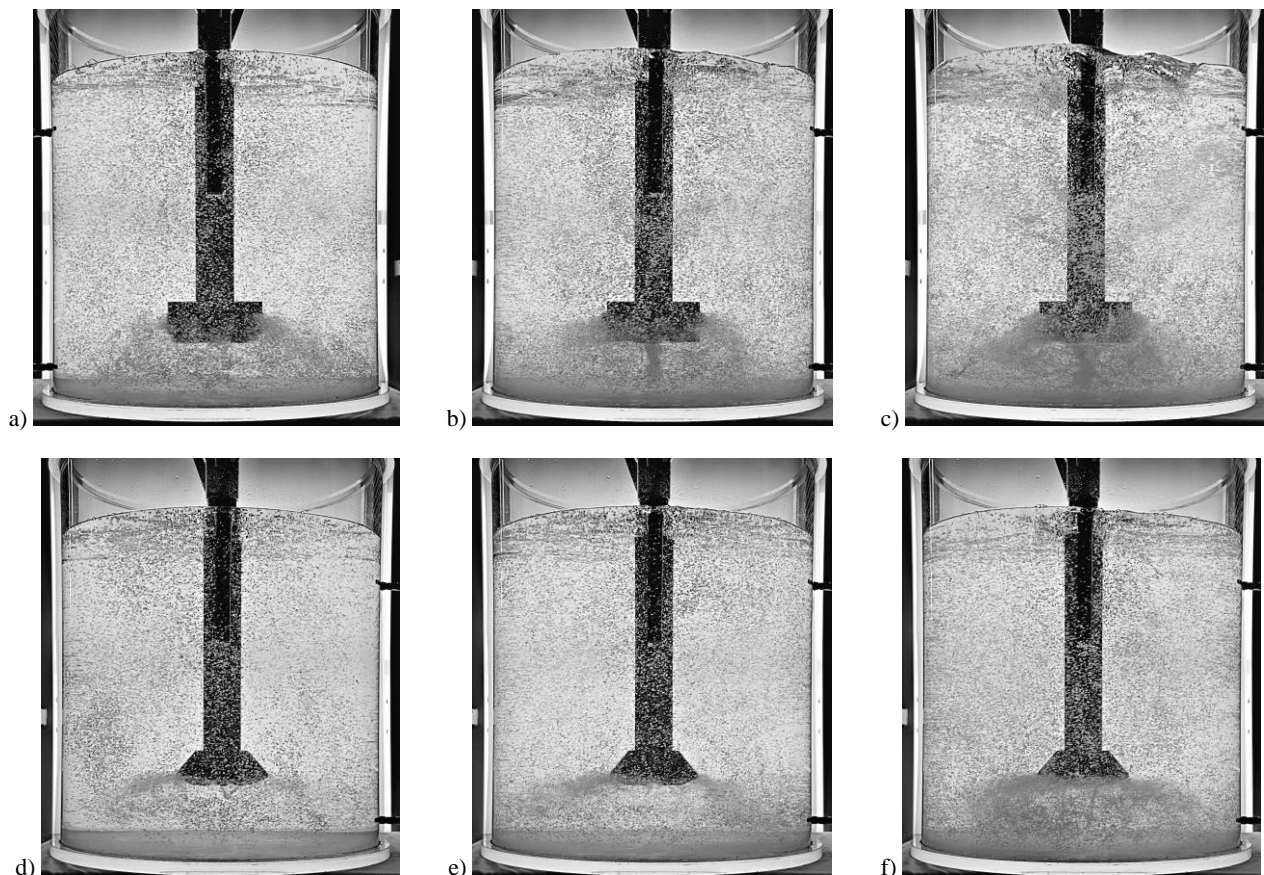


Fig. 7. Visualization images of the flow of gas in the bath at the volume flow rate of inert gas of 10 NL·min<sup>-1</sup>: (a) F2A 190 – 350 rpm, (b) F2A 190 – 500 rpm, (c) F2A 190 – 650 rpm, (d) J8 190 – 350 rpm, (e) J8 190 – 500 rpm, (f) J8 190 – 650 rpm [10]

In these photos, the effect of increasing rotary speeds that range from 350 to 650 rpm is evident, with the more intense distribution of bubbles throughout the refining ladle volume, as well as a higher level of bath surface ripple in the refining ladle.

With the impeller F2A 190, intense swirling and increased bubble concentration can be observed not only on the sides of the impeller but also below it, especially at higher rotary speeds. The formation of an intense vortex is also visible under the impeller, and in regular cycles also large rotating cavities that are filled with inert gas. These cavities break at about three-second intervals and then divide into a large number of small bubbles.

With the impeller J8 190, we can also observe the formation of cavities that are filled with inert gas, even at low rotary speeds of 350 rpm. If the size of the rotating cavity exceeds the critical

size, the cavity will break to form a large number of small bubbles.

Attention was also paid in the visualization experiments to the influence of the distance of the impeller from the bottom of the refining ladle (see Figure 8). The evaluation of the course of the dissolved oxygen content showed that the increase of this distance from 150 to 250 mm was reflected in a decrease in the efficiency of refining, respectively, in increasing refining times.

A possible explanation can be, as follows. At low rotary speeds, large bubbles form, which arise in the immediate vicinity of the impeller and then float to the surface. By shifting the point of formation of these bubbles by another 100 mm upwards, the volume of melt that is able to react with the bubbles of inert gas is reduced, which leads to increased melt turbulence and vortex formation, this difference in efficiency decreases.

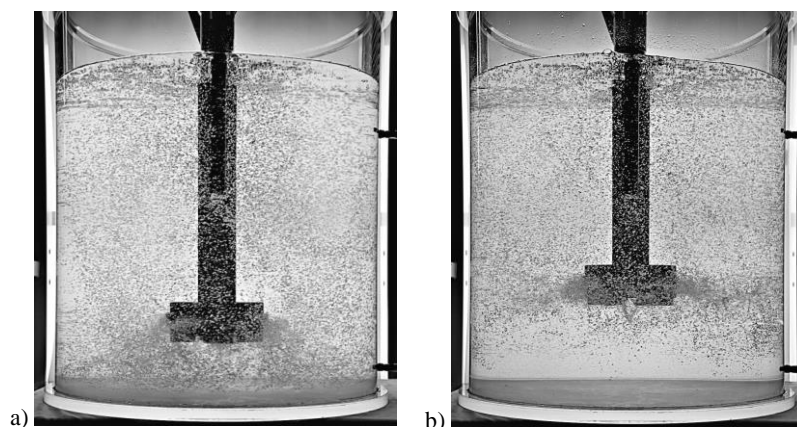


Fig. 8. Visualization images of the comparison of the bath behaviour in the ladle under the same conditions at the distance of the impeller from the bottom of the ladle: (a) 150 mm, (b) 250 mm [10]

## 4. Conclusions

Degassing (a reduction of hydrogen content) in aluminium-based melts was simulated in physical modelling by the process of reducing the dissolved oxygen content in water at a temperature of 20 °C. Its concentration in the water bath was measured while using two fluorescent probes.

The experiments were conducted under laboratory experiments in order to determine and evaluate the effect of each parameter on the efficiency of the melt refining process. The ability to influence the efficiency of the process was compared for individual parameters. These parameters include the geometry of the impeller, the height of the impeller above the bottom of the ladle, the volume flow rate of inert gas and the rotary impeller speed.

The evaluation of the experiments was carried out in three phases. In the first phase, experiments were performed, which were focused on the influence of individual parameters on the behaviour of oxygen during refining, which was then used to create combined graphs. In the second phase, the results were compared on the basis of the time to reach the dimensionless concentration of 0.5 and 0.1 in the bath. In the last phase, visualization photos were taken, where the size of the bubbles and the arrangement of these bubbles in the volume of the refining ladle were examined.

Based on the results obtained from experimental measurements the following findings can be formulated:

The rotary impeller speed has a very significant effect on the efficiency of the whole bath degassing process. The increased flow rate of inert gas also has an influence.

The comparison of impellers F2A 190 and J8 190 shows that the impeller F2A 190 achieved better results than the impeller J8 190 under all of the experimental conditions. This is mainly due to the geometry of the impeller.

The results clearly show that the increase in the distance of the impeller from the bottom of the ladle from 150 to 250 mm was reflected in a decrease in refining efficiency, respectively, in increasing refining times.

The comparison of values  $\tau_{0.5}$  a  $\tau_{0.1}$ , i.e. times during which the oxygen concentration in the bath was decreased to 50% resp. 10% of the initial value, led to the conclusion that the better results were achieved by the impeller type F2A 190.

During the experiments, photos of the bath behaviour inside the model were taken. The effect of increasing rotary speeds that range from 350 to 650 rpm is evident, with the more intense distribution of bubbles throughout the refining ladle volume.

Excessive rotary impeller speed increases can have a negative effect on the entrainment of non-metallic inclusions into the

aluminum melt. A vortex can also form under the rotor, disrupting the lining of the bottom of the ladle.

It is appropriate to mention that aluminium and water have rather different surface tensions and also that liquid aluminum surface is always covered by a slag, which may affect the results obtained in practical conditions. It would be appropriate to pay attention to this fact in the next model study.

## Acknowledgements

This research was funded with the support of the Czech Ministry of Industry and Trade within the frame of the programme TRIO within the solution of the project reg. No. FV10080 “Research and Development of Advanced Refining Technologies of Aluminium Melts for Increase in Product Quality”. The article was created thanks to the project No. CZ.02.1.01/0.0/0.0/17\_049/0008399 from the EU and CR financial funds provided by the Operational Programme Research, Development and Education, Call 02\_17\_049 Long-Term Intersectoral Cooperation for ITI, Managing Authority: Czech Republic-Ministry of Education, Youth and Sports. This work was also supported by the Student Grant Competition No. SP2022/15, SP2022/68 and SP2022/84.

## References

- [1] Michalek, K., Tkadlečková, M., Socha, L., Gryc, K., Saternus, M., Pieprzyca, J. & Merder, T. (2018). Physical modelling of degassing process by blowing of inert gas. *Archives of Metallurgy and Materials*. 63(2), 987-992. DOI: 10.24425/122432.
- [2] Hernández-Hernández, M., Camacho-Martínez, J., González-Rivera, C. & Ramírez-Argáez, M.A. (2016). Impeller design assisted by physical modelling and pilot plant trials. *Journal of Materials Processing Technology*. 236, 1-8. DOI: 10.1016/j.jmatprotec.2016.04.031.
- [3] Mostafei, M., Ghodabi, M., Eisaabadi, G.B., Uludag, M. & Tiryakioglu, M. (2016). Evaluation of the effects rotary degassing process variables on the quality of A357 aluminium alloy castings. *Metallurgical and Materials Transactions B*. 47(6), 3469-3475. DOI: 10.1017/s11663-016-0786-7.
- [4] Merder, T., Saternus, M. & Warzecha, P. (2014). Possibilities of 3D Model application in the process of aluminium refining in the unit with rotary impeller. *Archives of Metallurgy and Materials*. 59(2), 789-794. DOI: 10.2478/amm-2014-0134.
- [5] Saternus, M., Merder, T. & Pieprzyca, J. (2015). The influence of impeller geometry on the gas bubbles dispersion in URO-200 reactor – RTD curves. *Archives of Metallurgy and Materials*. 60(4), 2887-2893. DOI: 10.1515/amm-2015-0461.
- [6] Yamamoto, T., Suzuki, A., Komarov, S.V. & Ishiwata, Y. (2018). Investigation of impeller design and flow structures in mechanical stirring of molten aluminium. *Journal of Materials Processing Technology*. 261, 164-172. DOI: 10.1016/j.jmatprotec.2018.06.012.
- [7] Gao, G., Wang, M., Shi, D. & Kang, Y. (2019). Simulation of bubble behavior in a water physical model of an aluminium degassing ladle unit employing compound technique of rotary blowing and ultrasonic. *Metallurgical and Materials Transactions B*. 50(4), 1997-2005. DOI: 10.1017/j.s11663-019-01607-y.
- [8] Yu, S., Zou, Z.-S., Shao, L. & Louhenkilpi, S. (2017). A theoretical scaling equation for designing physical modelling of gas-liquid flow in metallurgical ladles. *Steel Research International*. 88(1), 1600156. DOI: 10.1002/srin.201600156.
- [9] Abreu-López, D., Dutta, A., Camacho-Martínez, J.L., Trápaga-Martínez, G. & Ramírez-Argáez, M. A. (2018). Mass transfer study of a batch aluminium degassing ladle with multiple designs of rotating impellers. *JOM*. 70, 2958-2967. DOI: 10.1007/s11837-018-3147-y.
- [10] Walek, J., Michalek, K., Tkadlečková, M. & Saternus, M. (2021). Modelling of technological parameters of aluminium melt refining in the ladle by blowing of inert gas through the rotating impeller. *Metals*. 11(2), 284. DOI: 10.3390/met11020284.
- [11] Saternus, M. & Merder, T. (2018). Physical modelling of aluminium refining process conducted in batch reactor with rotary impeller. *Metals*. 8(9), 726. DOI: 10.3390/met8090726.
- [12] Lichý, P., Bajarová, M., Kroupová, I. & Obzina, T. (2020). Refining aluminium-alloy melts with graphite rotors. *Materiali in Technologije*. 54(2), 263-265. DOI: 10.17222/mit.2019.147.
- [13] Lichý, P., Kroupová, I., Radkovský, F. & Nguyenová, I. (2016). Possibilities of the controlled gasification of aluminium alloys for eliminating the casting defects. 25<sup>th</sup> Anniversary International Conference on Metallurgy and Materials, May 25<sup>th</sup> - 27<sup>th</sup> 2016 (1474-1479). Hotel Voroněž I, Brno, Czech Republic, EU: Lichý, P.